Hydrological Sciences Journal
Publication details, including instructions for authors and subscription information:
http://www.tandfonline.com/loi/thsj20

Empirical Statistical Characterisation and Regionalisation of Amplitude-Duration-Frequency Curves for Extreme Peak Flows in the Lake Victoria Basin

Onyutha Charles[a] & Willems Patrick[ab]

[a] Hydraulics Laboratory, Katholieke Universiteit Leuven, Kasteelpark Arenberg 40, Leuven B-3001, Belgium

[b] Department of Hydrology and Hydraulic Engineering, Vrije Universiteit Brussel, Pleinlaan 2, Elsene, Brussel 1050, Belgium

Accepted author version posted online: 06 Mar 2014.

Empirical Statistical Characterisation and Regionalisation of Amplitude-Duration-Frequency Curves for Extreme Peak Flows in the Lake Victoria Basin

Onyutha Charles[1*] and Willems Patrick[1,2#]

[1]*Hydraulics Laboratory, Katholieke Universiteit Leuven, Kasteelpark Arenberg 40, Leuven B-3001, Belgium*
[2]*Department of Hydrology and Hydraulic Engineering, Vrije Universiteit Brussel, Pleinlaan 2, Elsene, Brussel 1050, Belgium*
*Charles.Onyutha@bwk.kuleuven.be
#Patrick.Willems@bwk.kuleuven.be

Received dd mm 20xx; accepted dd mm 20xx; open for discussion until dd mm 20xx

Citation Onyutha, C. and Willems, P., 20xx. Empirical Statistical Characterisation and Regionalisation of Amplitude-Duration-Frequency Curves for Extreme Peak Flows in the Lake Victoria Basin. *Hydrological Sciences Journal*, xx(x), xx–xx.

Abstract This paper focuses on a regionalisation attempt to partly solve data limitation problems in statistical analysis of high flows to derive discharge-duration-frequency (QDF) relationships. The analysis is based on 24 selected catchments in the Lake Victoria basin (LVB) in Eastern Africa. Characteristics of the theoretical QDF relationships were parameterized so as to capture their slopes (γ_{evd}) of extreme value distributions (EVD), tail behaviour (β) and scaling measures (α_s). To enable QDF estimates to be obtained for ungauged catchments, interdependency relationships between the QDF parameters were indentified and regional regression models were developed to explain the regional difference in these parameters from physiographic characteristics. In validation of the regression models, from the lowest (5 years) up to the highest (25 years) return periods considered, the percentage bias in the QDF estimates range from -2 % for 5 years return period up to 27 % for 25 years.

Key words extreme value analysis; flow extremes; floods; QDF; regionalisation

1. Introduction

Lake Victoria is the world's second largest freshwater lake situated at an altitude of 1134 m above sea level (m.a.s.l.). It has relatively small drainage basin which is slightly less than three times the lake's surface in area (Figure 1). The Lake's basin stretches 355 km in east-west direction (31°37' E to 34°53' E) and 412 km in north-south direction (00°30' N to 3°12' S). It has a shoreline of 4,828 km, a surface area of 68,800 km^2 and a total catchment area of about 184,000 km^2. With substantial rainfall that normally occurs throughout the year, more especially over the lake surface, the climate of Lake Victoria basin (LVB) may generally be described to vary from modified equatorial to semi-arid type. Low-lying parts of the LVB and areas close to Lake Victoria are normally characterized by episodes of floods, for instance, downstream of River Nzoia, around Budalang'i (Gichere et al. 2013). Hence there is a need for frequency analysis of such episodes, which requires an accurate descriptive study of hydrological extremes and their recurrence rates based on long-term time series of observations of rainfall intensities, discharges or water levels. An important way of obtaining substantially compressed

*conyutha@gmail.com , Tel: +32 485 55 32 32, Belgium, (Charles Onyutha)

information from a hydrological time series is through extreme value analysis for a range of aggregation levels to constitute relationships for Amplitude-Duration-Frequency. This relationship can be called discharge or Intensity-Duration-Frequency (QDF or IDF) for discharges or rainfall respectively. Aggregation levels are simply durational intervals over which the discharge or rainfall intensities are averaged or aggregated. According to World Meteorological Organization, WMO (2008), temporal aggregation of hydrological time series over several durations importantly removes short-term fluctuations to allow study of the general behaviour providing useful summary of the data to form basis of statistical analysis. Premised on such durations, the conditional relationships are essentially extreme value distributions (EVD) of the amplitude values in the time series (Chow et al. 1988). Importance of Amplitude-Duration-Frequency relationships is numerous in water engineering including planning, design, operation and/or management of water supply projects (e.g. dikes, dams, irrigation systems) (Nhat et al. 2006) or urban drainage facilities such as sewer conduits. According to Chow et al. (1988) and WMO (2009) Amplitude-Duration-Frequency relationships are also used to construct design storms for hydrological modelling applications.

Unfortunately, data limitation of the historical time series in the LVB is a major setback to such a study. Over reasonable areas of the LVB, either the catchments are ungauged, or gauged stations are not continuously operational due to poor maintenance. This data limitation creates high uncertainty in the calibration of the appropriate EVD. One of the approaches that can be used to partly solve the data limitation problem is regionalisation through regression models (as the form in Equation 2), which are constructed from basin characteristics or climatic variables. Such approach was used by the United States Geological Survey (USGS) as summarised in Jennings et al. (1994). According to Smakhtin (2001), the most commonly used basin and climate characteristics include: catchment area, mean annual precipitation, channel and/or catchment slope, stream frequency and/or density, percentage of lakes and forested areas, various soil and geology indices, length of the main stream, catchment shape and watershed perimeter, and mean catchment elevation. Regression models using a number of catchment characteristics were also developed in streamflow analysis in Australia by Nathan and McMahon (1991, 1992). Garcia-Martino et al. (1996) developed statistical models for streamflow estimation in Puerto Rico using selected basin characteristics including drainage density, the ratio of the length of tributaries to the length of the main channel, the percentage of drainage area with northeast aspect, and the average weighted slope.

This study implemented and tested a regionalisation attempt in statistical analysis of high flows to derive QDF relationships. The analysis is based on 24 selected catchments in the LVB, which is part of the upper White Nile basin. To enhance statistical accuracy and efficiency of the study findings and/or conclusions, emphasis was put on long-term discharge time series, preferably above 25 years. Six additional catchments, with more limited flow records were considered for the validation of the regional QDF model (see Table 1).

Figure 1 shows the locations of the discharge measurement stations used in this study and Table 1 shows for the selected catchments, some characteristics including flow record lengths, mean flow, locations and the physiographic characteristics.

>> INSERT Table 1

>> INSERT Figure 1

2. Methodology

2.1. QDF modelling

The extreme value analysis and QDF modelling are based on nearly independent extremes (peak values) extracted from daily full time series. This is done using independence criteria based on threshold values for the time difference between two successive independent peaks, the ratio of the minimum value between the two peaks over the peak value, and the peak height; see Willems (2009) for details on the method.

Prior to the extraction of the extreme values from the full time series for each of the selected stations, *n*-day moving averaging window was passed through the series. Aggregation levels of 1 day up to 1 year were considered. This is the range covered by multipurpose applications (e.g. agricultural, irrigation, power plants, domestic water supply, pollution etc). To come up with the Amplitude-Duration-Frequency relationships, for the selected range of aggregation levels, extreme value analysis was carried out and the suitable EVD was selected. To enable an adequate selection of the most optimal threshold level and to avoid systematic over/under-estimation in the tail of the distribution, quantile plots or Q-Q plots were considered. The same principle of calibrating the EVDs by a weighted linear regression in the Q-Q plot suggested by Csörgö et al. (1985) and Beirlant et al. (1996) and used by Willems et al. (2007), Taye and Willems (2011), Onyutha (2012), and Onyutha and Willems (2013) was adopted for this study. The extreme value index γ_{evd} (or $k = -\gamma_{evd}$), which is a parameter in the Generalised Extreme Value (GEV) distribution of Jenkinson (1955) or Generalised Pareto Distribution (GPD) of Pickands (1975), enables identification of the shape of the EVD. The class of the GEV distribution or GPD is identified as heavy tail (when $\gamma_{evd} > 0$ or $k < 0$), normal tail (when $\gamma_{evd} = k = 0$) and light tail (when $\gamma_{evd} < 0$ or $k > 0$). The weighting factors proposed by Hill (1975) were considered.

Figure 2 shows examples of calibrated EVDs as linear regression lines in exponential Q-Q plots. As explained in Beirlant et al. (1996) and Willems et al. (2007), linear upper tail behaviour as in Figure 2 means that the tail can be described by an exponential EVD (which is a special case of the GPD with zero shape parameter):

$$Q_T = \beta\,(\log(T) - \log(T_0)) + Q_{T0} \quad (1)$$

where, Q_T : the discharge (m^3s^{-1}) of return period, T (years)
T_0 : the return period which is equal or higher than that of the threshold event
Q_{T0} : the discharge (m^3s^{-1}) of return period, T_0 (years)
β : the slope (scale parameter) of the exponential EVD

>> INSERT Figure 2

Due to the fact that high fluctuations occur in the slope of the Q-Q plots (e.g. in Figure 3) for high thresholds due to randomness of the dataset, the slope estimates for these high thresholds have high statistical uncertainty. Instead for very low thresholds the slope estimates might result in pronounced bias (see the increasing slope on the right side of Figure 3b). The selection of optimal threshold values x_t above which the distributions are calibrated were ensured to be at points above which the mean squared error (E_{MS}) of the linear regression is minimal, i.e. within nearly horizontal sections in the plot of the slope versus the number of observations above threshold. For the examples of the daily flows of Nyando river (station 1GD01) and Nzoia river (station 1EF01), the optimal thresholds are determined as the flow values with threshold ranks t = 59 and t = 118 (i.e. the 59th and 118th highest flow values) as shown in Figure 3, plots a and b, respectively. A linear tail behaviour in the exponential Q-Q plot was obtained towards the higher Q values.

>> INSERT Figure 3

What followed next after carefully selecting, in a consistent way, the optimal thresholds for the different aggregation levels, was the calibration of the parameters of the EVD and analysis of the relationship between the model parameters and the aggregation levels as in Onyutha and Willems (2013). To derive smooth mathematical relationships, little but acceptable modifications were made to the model parameters. The parameter/aggregation level relationships, together with the analytical description of the EVD, finally constituted the QDF relationships as is shown next.

2.2. Parameterisation

To capture the differences in the characteristics of the QDFs for the selected stations, a number of parameters were derived as discussed below.

2.2.1. Parameter α_s

For catchments a, b, c, …., z and a particular T, we can have corresponding flow quantiles $Q_{a[T]}$, $Q_{b[T]}$, $Q_{c[T]}$, ……, $Q_{z[T]}$. If a point of reference, say flow quantile $Q_{R[T]}$, is selected, the differences ($Q_{a[T]}$-$Q_{R[T]}$), ($Q_{b[T]}$-$Q_{R[T]}$), ($Q_{c[T]}$-$Q_{R[T]}$), ….., ($Q_{z[T]}$-$Q_{R[T]}$) define parameters $\alpha_{a[T]}$, $\alpha_{b[T]}$, $\alpha_{c[T]}$, …., $\alpha_{z[T]}$ respectively. Parameter α_s indicates by how much the extreme values, i.e. flow quantiles, described by a QDF relationship have to be brought onto common curve for the region; in other words, it is a scaling measure. This parameter quantifies the site to site variation in hydrological events. This variation can be ascribed to the size of the catchment, the local climate, e.g. rainfall statistics, the catchment's land use, its topography, etc. The higher the value of parameter α_s, the higher are the flow extremes. This means that parameter α_s controls the magnitude of the runoff values. However, it is important to note that the basis for the choice of the reference curve to obtain parameter α_s is subjective. In this study, α_s was taken as the flow quantile for the 1-day aggregation level for all the selected catchments as illustrated in Figure 4. With increase in the return period, the value of α_s increases.

>>INSERT Figure 4

2.2.2. Parameter γ

Parameter γ is the slope of a QDF curve for a particular return period (see Figure 4). The value of this parameter is negative for high flow QDFs. It defines how strong the temporal variability in river flows is reduced by temporally aggregating the series. It can be taken to be an indicator of the dryness or duration of dry spells of the catchment under study. A more negative γ value indicates higher intermittency in the daily flows i.e. the existence of longer dry spells or stronger wet-dry variations while a less negative value of γ indicates higher temporal homogeneity in the streamflow of the catchment under consideration. Hence parameter γ also reflects the runoff variability over the catchment.

2.2.3. Parameters β

Parameter β is the slope of the EVD in an exponential Q-Q plot (see Equation 1). Note that for the exponential EVD, the relation between the extreme flow quantile and the reduced variate (here in this paper taken to be log-transformed return period) is linear. This means that for the same difference in log-transformed return periods (or log-frequency range), the same value for the difference between any two successive T-year curves on QDF relationship is obtained. It is this parameter β that determines how far apart the T-year curves for any selected successive return periods on QDF relationships can be. In this paper, this parameter β was considered at the 1-day aggregation level in the QDF relationships. A higher value of β means higher extreme flow variations. Important to note is that, when the scaling parameter α_s is known for a given return period, the scaling parameter can be computed for other return periods using β.

2.3. Analysis of correlative relationships between the QDF parameters

The relationships between the parameters derived from the theoretical QDFs were examined. The coefficient of determination, R^2 was used to judge the goodness-of-fits for the correlative relationships. The main idea here is that, in case of the existence of some correlative relationships between the QDF parameters, advantage can be taken on the interdependency to avoid the regional regression models being developed for each parameter.

2.4. Regression models

In support of the regionalisation approach, a search is done for physiographic or hydroclimatic characteristics that explain the variations in the parameters characterising the QDF relationships of the selected catchments. If such explanatory characteristics can be found, they can be used as predictors in regression models of the QDF parameters α_s, γ and β. These models would make it possible for ungauged catchments to estimate their QDF relationships. According to Downer (1981), development of a better understanding of the physical factors affecting the streamflow can help to enhance the accuracy of regression models. The most important step in the build-up of the regional regression models entailed the careful selection of the predictor variables. In this study, the following catchment characteristics were considered: catchment area (A_R, km^2), mean

point catchment slope (S_L, %), mean annual rainfall (R_{AM}, mm), mean annual potential evapotranspiration (E_{MAT}, mm), closest distance to the Lake Victoria shoreline (DL, km), the mean point elevation (E_{LEV}, m.a.s.l.), and the aspect (A_{SP}, -). S_L and E_{LEV} were selected because they determine the catchment response to runoff. D_L captures the hydroclimatic influence of Lake Victoria on the surrounding catchments in the study area. Catchment rainfall intensity determines the magnitude of hydrological extreme events. A_{SP} reflects the direction of catchment runoff, i.e. the bearing of Lake Victoria from a particular catchment in question. S_L, A_{SP} and E_{LEV} were each estimated from the 90 m x 90 m digital elevation model (DEM) by averaging 100 randomly selected points in the catchment area upstream of a given measurement station. The Hole-filled DEM derived from the USGS/NASA (Jarvis et al. 2008) and processed by the International Centre for Tropical Agriculture (CIAT-CSI-SRTM) using interpolation methods described by Reuter et al. (2007) was used in this study. In a trial and error procedure, jointly for all the selected catchments of the study area, correlative relationships of α_s, γ and β with the physiographic and/or hydroclimatic characteristics were examined through scatter plots. Multivariate regression models entailing the multiplicative relationships were tested. The multiplicative model takes the following form:

$$\rho = a_o \left(P_1\right)^{a_1} \left(P_2\right)^{a_2} .... \left(P_n\right)^{a_n} \quad (2)$$

where, ρ : the parameter to be predicted
a_j : regression coefficients, $j = 0, 1, 2, \ldots, n$
P_i : the predictor, $i = 0, 1, 2, \ldots, n$

Such multiplicative relationship was also considered by Stedinger et al. (1993) for the prediction of flood quantile estimates based on physiographic and climate characteristics. The expression of the form as in Equation 2 was also included by the Federal Highway Administration, FHWA (1996) in the Urban Drainage Design Manual for estimating peak flows from basin characteristics. In this study, the multiplicative combination with the least number of physiographic and/or hydro climatic characteristics giving partial correlation of at least 0.4 with a particular parameter of the QDF relationship was adopted as a predictor.

In the calibration procedure, all the 24 selected catchments were jointly used for a selected return period. During the calibration, the evaluative 'goodness-of-fit' analysis was both graphically and statistically done. Statistically, so as to achieve a high value of R^2, adding more variables might be an option one would wish to undertake irrespective of whether the added variables are relevant or not. This trick is not encouraging but rather misleading, and consequentially an adjusted R^2 ($\hat{R}^2$) was used in this study since it considers some punitive measure attached to addition of more variables. Out of the various formulae outlined by Snyder and Lawson (1993) and Yin and Fan (2001), which shrink R^2 based on the number of predictors (v), sample size (n), and the obtained effect (R^2) as an initial estimate of the population effect, Leach and Henson (2007) empirically evaluated the reporting of adjusted effect sizes (e.g. adjusted R^2) in published multiple regression studies. They identified the types of corrected effects reported, and found out that, out of the several adjusted R^2 formulae, the formula of Ezekiel (1930) expressed in Equation 3 provided the most conservative correction for sampling error.

The Ezekiel (1930) formula, which can reasonably be confused with that of Wherry (1931), is actually a modification of that for Ezekiel (1929). The Ezekiel (1930) formula as expressed in Equation 3 was used in this study.

$$\hat{R}^2 = 1 - \frac{(n-1)}{(n-v-1)}\left(1 - R^2\right) \tag{3}$$

where, $\hat{R}^2$: adjusted R^2
R^2 : coefficient of determination

Statistical goodness-of-fits of the calibrations were also evaluated using the model efficiency coefficient (E_F). The popular E_F of Nash and Sutcliffe (1970) which is given by Equation 4 is a dimensionless and scaled version of the mean squared error (E_{MS}) and varies from 1 (indicating the best model performance) to negative infinity.

In a trial and error procedure, the regression parameters were at first, manually adjusted till the highest possible value of $\hat{R}^2$ was achieved. In a fine-tuning step, optimisation technique of E_{MS} minimisation was adopted. At this point, the computed standard error of regression estimates (S_e), which is actually the standard deviation of the predicted values of γ was expected to be at its minimum.

2.5. Uncertainty and analysis of errors

After calibration, validation of the regression models was conducted based on six discharge measurement stations with short records of data (see Table 1). In this validation step, model performance was evaluated based on the model bias (B_{ias}) and the root mean square of the model residual error (E_{RMS}). Considering i to be the rank of the selected aggregation levels of the study (i = 1 for the lowest i.e. 1 day); H the number of aggregation levels; $M_{p,i}$ the theoretical quantile at i; $M_{e,i}$ the empirical quantile at i; $\bar{M}_p$; the mean of theoretical quantiles; the mean of values obtained from expression ($M_{p,i}$ - $M_{e,i}$) as percentage of $M_{e,i}$ for i = 1 to H is considered the average percentage bias as in Equation 5. For an ideal model, the B_{ias} [%] is equal to zero and the model is said to be unbiased. The overall differences between $M_{e,i}$ and $M_{p,i}$ values of each catchment were also evaluated in terms the relative root mean squared error E_{RMS} (Equation 6).

$$E_F[-] = 1 - \left[\frac{\sum_{i=1}^{H}\left(M_{e,i} - M_{p,i}\right)^2}{\sum_{i=1}^{H}\left(M_{p,i} - \bar{M}_p\right)^2}\right] \tag{4}$$

$$B_{ias}\,[\%] = \frac{1}{H}\sum_{i=1}^{H}\left(\frac{M_{p,i} - M_{e,i}}{M_{e,i}} \times 100\right) \tag{5}$$

$$E_{RMS}\ [\mathrm{m^3 s^{-1}}] = \left(\frac{1}{H}\sum_{i=1}^{H}(M_{p,i} - M_{e,i})^2\right)^{0.5} \tag{6}$$

Since there were no empirical values in the QDFs for return periods higher than the length of the available flow series, the goodness-of-fit of flow quantiles had to be validated for the lower return periods of 5, 10, 15, 20 and 25 years. Using the empirical and theoretical daily discharges from the QDF relationships of all the selected stations, the B_{ias} [%] and the E_{RMS} [m^3s^{-1}] for the aforementioned return periods were evaluated using Equations 5 and 6 respectively.

2.6. Validation of regression models

Ideally, *T*-year curves are to be parallel to each other on QDF relationships. This means that the deviations of parameter γ for the selected *T*-year curves on QDF relationships are expected to be minimal. Estimating QDF relationships in ungauged catchments taking into account the interdependency of the parameters of a QDF can be carried out using the steps below:

i) estimating parameter γ for a return period of 5 years using Equation 2
ii) Determining parameter β from its relationship with the estimated parameter γ
iii) Determining parameter α_s for a return period of 5 years from its relationship with β or γ
iv) Using the estimated parameters α_s and β to derive QDF relationships for return periods higher than 5 years (Equation 1).

3. Results and discussion

3.1. QDF models

Figure 5 shows examples of the QDF relationships obtained after compiling the exponential EVD calibration results for river flows aggregated over time scales of 1, 3, 5, 7, 10, 30, 45, 60 and 90 days, after parameterisation of the QDF relationships. Up to the length of the available time series, empirical quantiles were derived as well. Because the lengths of the available river flow series were all more than 25 years, empirical *T*-year events are only shown for curves up to 25 years in Figure 5. For higher return periods, due to the randomness involved in the empirical data, the empirical quantiles can be far more inaccurate in comparison with the theoretical quantiles. Differences between the empirical and theoretical quantiles can, for the higher return periods, also be explained by the influence of river flooding i.e. the difference between the river discharges and the catchment rainfall-runoff discharges.

>>INSERT Figure 5

Figure 6 shows the graphical goodness-of-fit of the flow quantiles after calibration of the EVDs for daily aggregation level; for return periods of 5, 10 and 25 years. Considering the full range of aggregation levels, low values of B_{ias} [%] and E_{RMS} [m^3s^{-1}] were realised for the calibrated *T*-year flow estimates as seen in Table 2. This means that, the fittings between empirical and theoretical points defining QDF relationships before parameterisation were highly acceptable.

>>INSERT Table 2

In practice, for design of hydraulic structures such as along sewer and river systems, bridges and culverts, return periods between 5 and 100 years are used. Higher return periods around T_{100} are used mainly for flood plain development, and medium-sized flood protection works. Although T_{500} is rarely used in designs, it was in this study used for the assessment of the reliability of the projected QDF discharges for extreme conditions through extrapolation of the EVD.

>> INSERT Figure 6

3.2. Relationships between the QDF parameters

Figure 7 indicates that, parameters α_s, γ and β all depend on each other. The following relationships were deduced:

$$\beta = -163.9344\,(\gamma_5) - 19.5738 \quad (7)$$

$$\alpha_5 = 0.2444\,(\beta) + 5.0624 \quad (8)$$

$$\gamma_5 = \frac{1}{414.5104}(\alpha_5 + 15.4309) \quad (9)$$

This dependency between the QDF parameters means that they all depend on the magnitude of the temporal variability in streamflow. For stations with higher temporal variability (stronger differences between low and high flows), parameter γ indicates a higher slope (more negative values; because of stronger differences between short-duration values and longer duration values), parameter α_s will be higher because extremes will be higher for small aggregation levels, and parameter β will be higher because of higher difference between low and high extremes. The parameters α_s and γ used to obtain Figure 7 and Equations 7 to 9 were picked from a return period of 5 years. Similar plots were however made with all the selected return periods of the QDF relationships. The values of R^2 in the regression between QDF parameters were noted to reduce with increase in the return periods due to the higher uncertainty in extreme value analysis for higher return periods.

>>INSERT Figure 7

3.3. Relating QDF parameters to physiographic and hydroclimatic catchment characteristics

As shown in Table 3, the R^2 values of the regression models between the QDF parameters and physiographic or hydroclimatic catchment characteristics are low when individual characteristics are considered as single predictor. However, the correlative relationships are largely enhanced when different catchment characteristics are combined through

multiplicative models of Equation 2. As shown in Table 4, highest R^2 values were obtained when A_R, and S_L are combined, thus when [A_R.S_L] or [A_R.S_L.R_{AM}] are used as predictor variable. Figure 8 shows the 5-year QDF parameters versus [A_R.S_L].

>>INSERT Table 3

>>INSERT Table 4

Table 5 shows values of R^2 for the relationships between QDF parameters and the predictor variable taken as [A_R.S_L] or [A_R.S_L.R_{AM}] with and without scaling exponents. For the models with scaling exponents, the final values of R^2 shown in Table 5 were again obtained after application of E_{MS} minimisation to obtain optimal sets of the regression coefficients. The difference in R^2 values obtained for the models with and without scaling exponents is small. Eventually, model $a_0(A_R.S_L)^{a1}$ was selected because it has lowest number of parameters among the models with highest R^2 values.

The careful combination of predictors is a plausible approach because it avoids overfitting resulting from multicollinearity and overparameterisation in the regression model. The calibrated regional regression models for T = 5 years can be seen in Figure 9 and Table 6. From Table 5 it can be seen that the values of the R^2 of the regression models reduce with increase in return periods. This again is due to the uncertainty boost in extreme value analysis as return periods increase.

>> INSERT Table 5

>> INSERT Figure 8

3.4. Regression model

Table 6 shows the regional regression model for the QDF parameter γ using the combined characteristic in the form $a_0(A_R.S_L)^{a1}$. The calibrated regional regression models were evaluated both graphically (Figure 9) and statistically (Table 6). The computed standard deviations (S_{tdev}) and standard error of regression estimates S_e, reflect the total uncertainty in the regression models. This uncertainty might be due to the incomplete model structure as well as the uncertainty in the statistical extreme value analysis and the river flow measurement errors.

>> INSERT Figure 9

>> INSERT Table 6

Since parameter γ was found to be correlated to both parameters α_s and β, regression model was developed only for γ of 5 years so that α_s and β can be estimated from their dependency relationship with γ.

The examined variation of the QDF parameters with return period can be seen to follow power curves tending to asymptotic behaviour with very high return periods (see Figure 10). The shapes of these curves were found to remain similar for all the catchments. The parameters α_s and γ smoothly vary with changing return period. The magnitude of parameter γ decreases as the return period increases; the reverse is true for parameter α_s (Figure 10).

>> INSERT Figure 10

3.5. Spatial variations in the QDF parameters and hydroclimatic variables

Figures 11 and 12 show the spatial variation of QDF parameters using R_{AM} and $A_R.S_L$. These maps were obtained by surface interpolation (krigging method) of the standardized QDF parameters β and α_s based on the 30 catchments. The spatial maps for R_{AM} and $A_R.S_L$ were obtained using observations from meteorological stations within and around the study area.

For ease of visualization of the similarities between maps a and b of Figure 11, areas with similar patterns have been encircled; this can be seen in the north eastern (C), eastern (A) and north western parts (B) of the basin. Of course, due to low spatial density of the network of stations, there are local influences from individual stations. For that reason, spatial similarities should not be compared at the level of individual stations but for larger areas. One possible solution to overcome this problem is to filter out the influence of local stations using stronger spatial smoothing, but this was not feasible due to the low stations' resolution in some regions such as the south western region around station e. There are some local inconsistent values which indicate that more reliable QDF fittings to yield consistent hydrological parameters such as α_s, γ and β for a given region can be deduced only when there are more discharge stations with available flow observations. The 24 discharge stations considered for the study might have been less than the required to obtain clear regional (spatial) variations of the parameters derived from the QDF relationships.

Region A in Figure 11 and Figure 12a shows higher α_s, β and γ values in the lower areas next to Lake Victoria, whereas the regions B and C show lower values. The higher values in region A are explained by the higher rainfall extreme intensities in that region, as shown in the Nile basin regional extreme value analysis by Nyeko-Ogiramoi et al. (2012). These higher intensities are also reflected in the higher R_{AM} values for that region (Figure 12a). In the south of region A around stations 4 and 10 the R_{AM} values are lower

but the QDF parameters α_s, β and γ remain high because of the higher $A_R.S_L$ values for these stations (sub-region D2, Figure 12b). For the same reason, similar pattern can be obtained in the north western area between stations 2 and 7 (sub-region D1, Figure 12b). Also the higher α_s value for station 6 is due to the higher catchment area. The lower QDF parameter values for regions B and C are explained by both lower rainfall volumes and lower $A_R.S_L$ values. The stations in the south such as stations 5, 9, 20, d and f also have low R_{AM} and $A_R.S_L$ values, but due to the higher E_{MAT} for that region (not shown), β and γ values are lower than that of regions B and C.

>> INSERT Figure 11 a)

>> INSERT Figure 11 b)

>> INSERT Figure 12 a)

>> INSERT Figure 12 b)

3.6. Validation of regional QDF models

Due to the fact that the validation stations were characterized by short data records (less than 12 years), the regional regression models were validated for return periods of 5, 10, 15, 20 and 25 years. This is because the short data records may cause high uncertainty in the statistical analysis of extreme events if used to estimate QDF relationships for very high return periods e.g. 100 or 500 years. Table 7 shows the overall B_{ias} [%] and E_{RMS} [m^3s^{-1}] in the QDF estimates. The overall B_{ias} [%] and E_{RMS} [m^3s^{-1}] values increase with increasing return period (see also Figure 14).

>>INSERT Table 7

From Table 7 it can be seen that for a return period of 5 years, the validation result is reasonably well. However, for higher return periods, significant overestimations are found. This might be due to uncertainties in both the empirical and theoretical flow quantiles, due to the uncertainty in the statistical extreme value analysis, and the flow measurement errors. There might also be the most important reason that, the validation periods are limited in their length; hence the empirical flow values might be biased from the longer term values due to the decadal or multi-decadal climate oscillations as shown in Taye and Willems (2011). Figure 13 shows the mean temporal variability (computed using a time slice of 5 years) for mean of annual maxima of river flows (R_{AMF}) of all the selected catchments of LVB in Table 1. The oscillation pattern of Figure 13 was calculated using the quantile anomaly indicator on which the details can be found fully discussed in Ntegeka and Willems (2008), and Willems (2013). Since the construction of QDF relationships is dependent on the periods used for the statistical analysis, the QDF

quantiles obtained are respectively higher and lower during the oscillation highs (OHs) and lows (OLs) in comparison with the use of long record data. They may lead to biases in the QDF quantiles when they are based on short data records. From Figure 13, it is shown that OHs in the mean of R_{AMF} of LVB occurred in the mid 1960s, the period between the late 1970s and early 1980s, and the 1990s. The OHs of the mid 1960s and the 1990s were significant at 5 % level of significance. The OLs were in the 1970s and the mid 1980s. It is also shown from Figure 13 that there was a steadily increasing trend from 1970 to 2000 at a rate of 0.909 % per year. If such temporal variations are significant, the applicability of the regional regression models may be lowered unless bias correction is applied in order to correct the QDF quantiles to account for the longer term flow variations. This can be done based on the anomaly indicator shown in Figure 13 as demonstrated by Taye and Willems (2011).

>>INSERT Figure 13

The significant overestimations in the validation result might also be the influence of flooding. It also might be due to the uncertainty in the developed regional regression models which have limited capacity to capture the site to site hydrological variations. If more stations with available data would become available, most likely the accuracy of the regional models could be largely improved. Another reason for the overestimations in the QDF estimates is that the predictors used in the regional regression models, i.e. A_R and S_L, are static in nature and may not adequately capture the changes in streamflow regimes in time. Improved regional regression models might also be obtained from regional regression analysis using data from hydroclimatic variables such as rainfall and evapotranspiration at smaller time steps, e.g. at daily resolutions.

Figure 14 shows evaluation of regional regression models for selected return periods. By considering the E_{RMS} as the measure of uncertainty in the QDF estimates, it can be seen that the E_{RMS} increases with increasing return periods (Figure 14). For all the return periods considered, the highest and the lowest E_{RMS} values were obtained for Kagera Nyakanyasi and Ngono Kalebe (i.e. the largest and the smallest catchments) respectively. The size of the catchment and the consequent order of magnitude of the streamflows thus have a strong influence on the accuracy of the QDF estimates.

>> INSERT Figure 14

4. Conclusions

This paper has provided a means of constructing estimates of QDF relationships for the hydrological extremes of ungauged catchments in the LVB for a number of applications including irrigation, hydropower supply, water supply, etc, to assess the water management requirements in terms of cumulative volumes of water available during high flows. This can be done based on specific aggregation levels or return periods depending on the application. Twenty four selected catchments in the study area were used to model and characterize QDF relationships so as to capture their slopes (γ), tail behaviour (β) of the EVD and scaling measures (α_s). The QDF parameters α_s, γ and β were found to depend on each other. Their spatial variability could be ascribed to site to site differences between the catchments with respect to the hydroclimatic (rainfall, evapotranspiration) and physiographic characteristics such as catchment area and slope. To explain the regional difference in the QDF parameters from these physiographic characteristics, regional regression models were obtained based on combined multiplicative relationships. Catchment area, slope and mean annual rainfall were found to have the highest correlations with the QDF parameters. The multiplicative combination of these three characteristics was found to present the highest correlative relationships with the QDF parameters with the R^2 values of 0.61, 0.44 and 0.52 for parameters α_s, γ and β respectively. For the multiplicative combination of area and slope, the R^2 values only reduced slightly. The regression model $a_0(A_R.S_L)^{a1}$ was selected because it has low number of parameters but high R^2 value. Application of scaling exponents to the individual catchment characteristics in the regression model did not show significant improvement in the model performance. From the calibration results, E_{RMS} [m^3s^{-1}] and B_{ias} [%] for modelled versus observed flow quantiles were found to be 0.23 m^3s^{-1} and 0.37 % respectively. The average percentage bias for all validation stations and aggregation levels considered is -2 % and 27 % for the lowest and highest return periods considered in the study, i.e. 5 and 25 years respectively.

It should be noted that the physiographic characteristics used in the regression models are static and may not adequately capture the changes in streamflow regimes with time. In determining the relationships between the streamflow QDF statistics and the physiographic and hydroclimatic characteristics, mean annual rainfall data was used. It is however expected that, improved models might be obtained from rainfall volumes during the wet seasons, or from daily rainfall based extreme value analysis. In the update of the regional regression models, more discharge measurement stations with up-to-date data could be used to fine tune the interdependency between the QDF parameters, and also the correlative relationships between parameters α_s, γ and β and the physiographic or hydroclimatic characteristics. Another interesting study would be to determine the variability in parameters α_s, γ and β and examine if they are correlated with the trends in land use of the study area; this would help to deduce a quantitative measure in the variability pattern for the parameters α_s, γ and β with respect to the anthropogenic influence.

5. Acknowledgment

The research was linked to the FRIEND/NILE project of UNESCO and the Flanders in Trust Fund. The historical discharge data were obtained at KU Leuven from the database

of the aforementioned project. The DEM used in this study was obtained online from the International Centre for Tropical Agriculture, CIAT-CSI SRTM website, http://strm.csi.cgiar.org/ [accessed 30th November, 2010].

6. References

Beirlant, J., Teugels, J.L. and Vynckier, P., 1996. *Practical analysis of extreme values*. Leuven, Belgium: University Press Leuven.

Chow, V.T., Maidment, D.R. and Mays, L.W., 1988. *Applied Hydrology*. New York, U.S.A: McGraw-Hill Book Company.

Csörgö, S., Deheuvels, P. and Mason, D., 1985. Kernel estimators of the tail index of a distribution. *Annals of Statistics*, 13, 1050–1077.

Downer, R.N., 1981. Low-flow studies for Vermont - a prognosis for success. Hydro Power and its Transmission in the Lake Champlain Basin. Proceedings of the Eighth Annual Lake Champlain Basin Environmental Conference, pp. 43–51.

Ezekiel, M., 1929. The application of the theory of error to multiple and curvilinear correlation. *American Statistical Association Journal*, 24, 99-104.

Ezekiel, M., 1930. *Methods of correlational analysis*. New York, U.S.A: John Wiley and Sons, Inc.

Federal Highway Administration, FHWA., 1996. Urban drainage design manual (SI), hydraulic engineering circular No. 22 (FHWA-SA-96-078), U.S Department of Transportation, Washington, DC, 478 pp.

Garcia-Martino, A.R., Scatena, F.N., Warner, G.S. and Civco, D.L., 1996. Statistical low-flow estimation using GIS analysis in humid montane regions in Puerto Rico. *Water Resources Bulletin*, 32(6), 1259–1271.

Gichere, S.K., Olado, G., Anyona, D.N., Matano, A.S., Dida, G.O., Abuom, P.O., Amayi, A.J. and Ofulla, A.V.O., 2013. Effects of drought and floods on crop and animal losses and socio-economic status of households in the Lake Victoria Basin of Kenya. *Journal of Emerging Trends in Economics and Management Sciences*, 4(1), 31–41.

Hill, B.M., 1975. A simple and general approach to inference about the tail of a distribution. *Annals of Statistics*, 3, 1163-1174.

Jarvis, A., Reuter, H.I., Nelson, A. and Guevara, E., 2008. *Hole-filled seamless SRTM data V4, International Centre for Tropical Agriculture (CIAT)* [online]. Available from: http://srtm.csi.cgiar.org [accessed on 30th November, 2010].

Jenkinson, A.F., 1955. The frequency distribution of the annual maximum (or minimum) of meteorological elements. *Quarterly Journal of the Royal Meteorological Society*, 81(348), 158-171.

Jennings, M.E., Thomas, Jr., W.O. and Riggs, H.C., 1994. Nationwide summary of U.S. Geological Survey regional regression equations for estimating magnitude and frequency of floods for ungaged sites, 1993. U.S. Geological Survey, water resources investigations report 94–4002, prepared in cooperation with the Federal Highway Administration and the Federal Emergency Management Agency, Reston Virginia.

Leach, F.L. and Henson, K.R., 2007. The use and impact of adjusted R^2 effects in published regression research. *Multiple Linear Regression Viewpoints*, 33(1), 1-11.

Nash, J.E. and Sutcliffe, I.V., 1970. River flow forecasting through conceptual models. *Journal of Hydrology*, 273, 282-290.

Nathan, R.J. and McMahon, T.A., 1991. Estimating low flow characteristics in ungauged catchments: a practical guide. Department of Civil and Agricultural Engineering, University of Melbourne, Australia, 60 pp.

Nathan, R.J. and McMahon, T.A., 1992. Estimating low flow characteristics in ungauged catchments. *Water Resources Management*, 6(2), 85–100.

Nhat, L.M., Tachikawa, Y. and Takara, K., 2006. Establishment of intensity-duration-frequency curves for precipitation in the monsoon area of Vietnam. *Annals of Disaster Prevention Research Institute Kyoto University*, 49, 93–103.

Ntegeka, V. and Willems, P., 2008. Trends and multidecadal oscillations in rainfall extremes, based on a more than 100-year time series of 10 min rainfall intensities at Uccle, Belgium. *Water Resources Research*, 44(7), W07402.

Nyeko-Ogiramoi, P.O., Willems, P., Mutua, F. and Moges, S.A., 2012. An elusive search for regional flood frequency estimates in the River Nile basin. *Hydrology and Earth System Sciences*, 16, 3149-3163.

Onyutha, C., 2012. Statistical modelling of FDC and return periods to characterise QDF and design threshold of hydrological extremes. *Journal of Urban and Environmental Engineering*, 6(2), 140–156.

Onyutha, C. and Willems, P., 2013. Uncertainties in flow-duration-frequency relationships of high and low flow extremes in Lake Victoria basin. *Water*, 5(4), 1561-1579.

Pickands, J., 1975. Statistical inference using extreme order statistics. *Annals of Statistics*, 3, 119-131.

Reuter, H.I., Nelson, A. and Jarvis, A., 2007. An evaluation of void filling interpolation methods for SRTM data. *International Journal of Geographic Information Science*, 21(9), 983-1008.

Smakhtin, V.U., 2001. Low flow hydrology: a review. *Journal of Hydrology*, 240, 147–186.

Snyder, P. and Lawson, S., 1993. Evaluating results using corrected and uncorrected effect size estimates. *Journal of Experimental Education*, 61, 334–349.

Stedinger, J.R., Vogel, R.M. and Foufoula-Georgiou, E., 1993. Frequency analysis of extreme events. *In*: D.R. Maidment, ed. *Handbook of Hydrology*. New York, U.S.A: McGraw-Hill, 18.1-18.66.

Taye, M.T. and Willems, P., 2011. Influence of climate variability on representative QDF predictions of the upper Blue Nile Basin. *Journal of Hydrology*, 411, 355-365.

Wherry, R.J., 1931. A new formula for predicting the shrinkage of the coefficient of multiple correlation. *Annals of Mathematical Statistics*, 2, 440-451.

Willems, P., Guillou, A. and Beirlant, J., 2007. Bias correction in hydrologic GPD based extreme value analysis by means of a slowly varying function. *Journal of Hydrology*, 338, 221-236.

Willlems, P., 2009. A time series tool to support the multi-criteria performance evaluation of rainfall-runoff models. *Environmental Modelling software*, 24(3), 311-321.

Willlems, P., 2013. Multidecadal oscillatory behaviour of rainfall extremes in Europe. *Climate Change*, 120, 931-944.

World Meteorological Organization, WMO., 2008. Hydrological data. *In*: Manual on low-flow estimation and prediction; Operational Hydrology Report No. 50, WMO-No.1029, Geneva, Switzerland, 138 pp.

World Meteorological Organization, WMO., 2009. Management of water resources and application of hydrological practices. *In*: Guide to Hydrological Practices, Volume II, Sixth Edition; WMO-No.168, Geneva, Switzerland, 302 pp.

Yin, P. and Fan, X., 2001. Estimating R^2 shrinkage in multiple regression: a comparison of analytical methods. *The Journal of Experimental Education*, 69, 203-224.

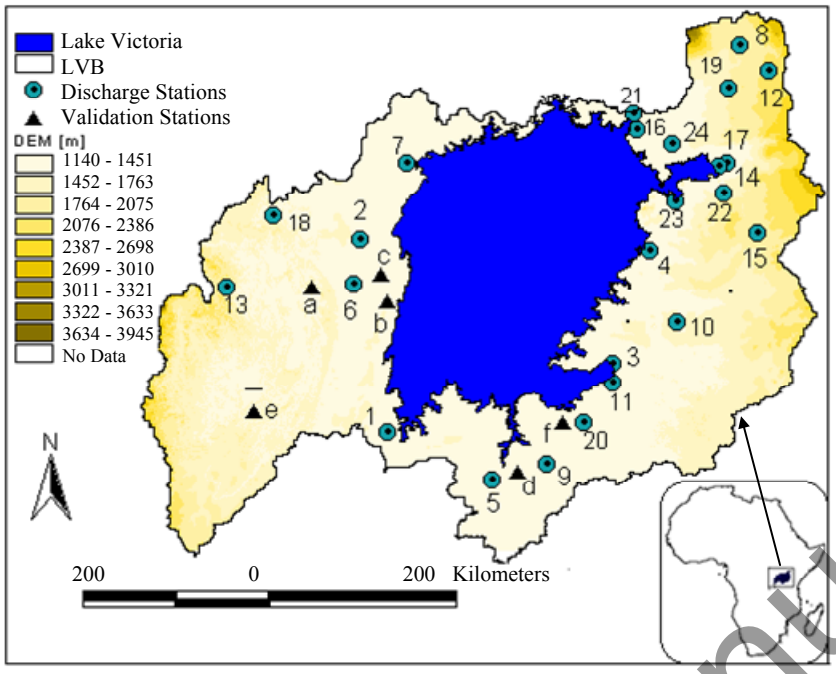

Figure 1 Lake Victoria Basin (LVB) showing locations of the discharge stations and validation stations (see Table 1 for the details).

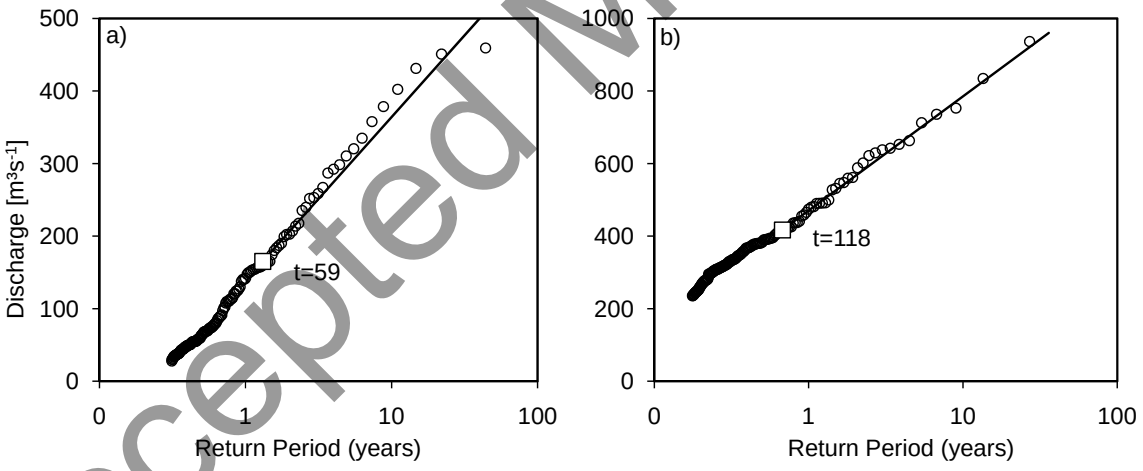

Figure 2 Observations (o) in exponential Q-Q plots of daily discharges; graph a) is for high flows in the Nyando river (station 1GD01) and b) is for high flows in the Nzoia river (station 1EF01). Symbol (□) denotes the selected optimal threshold; and the regression line is the calibrated EVD; the graphs share similar labelling for the vertical axes.

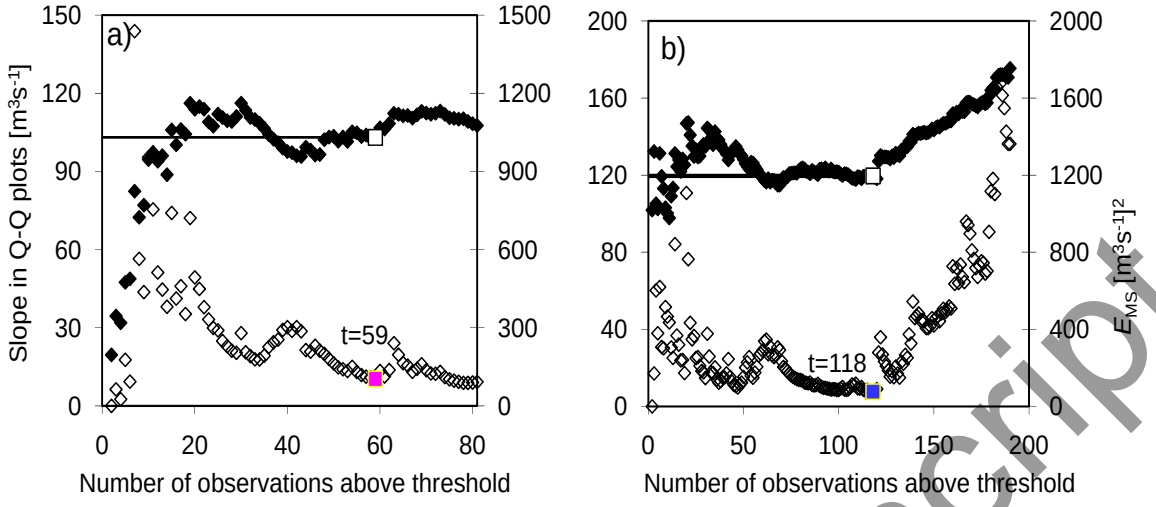

Figure 3 Left vertical axis (♦), Hill-type estimation of slope in the exponential Q-Q plot; right vertical axis (◊), mean squared error (E_{MS}) of Hill-type regression in the exponential Q-Q plot; (□) selected optimal threshold; the graphs a) and b) are for daily discharges of Nyando river (station 1GD01) and Nzoia river (station 1EF01) respectively. The graphs share same label for the vertical axes.

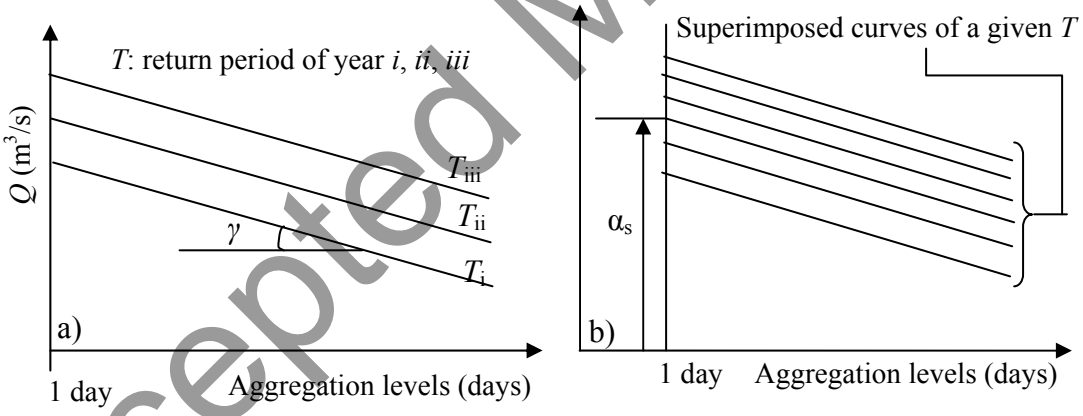

Figure 4 Parameters characterising the peak flow QDFs. Illustrations a) and b) are for parameters γ and α_s respectively. The charts share the same label for the vertical axis.

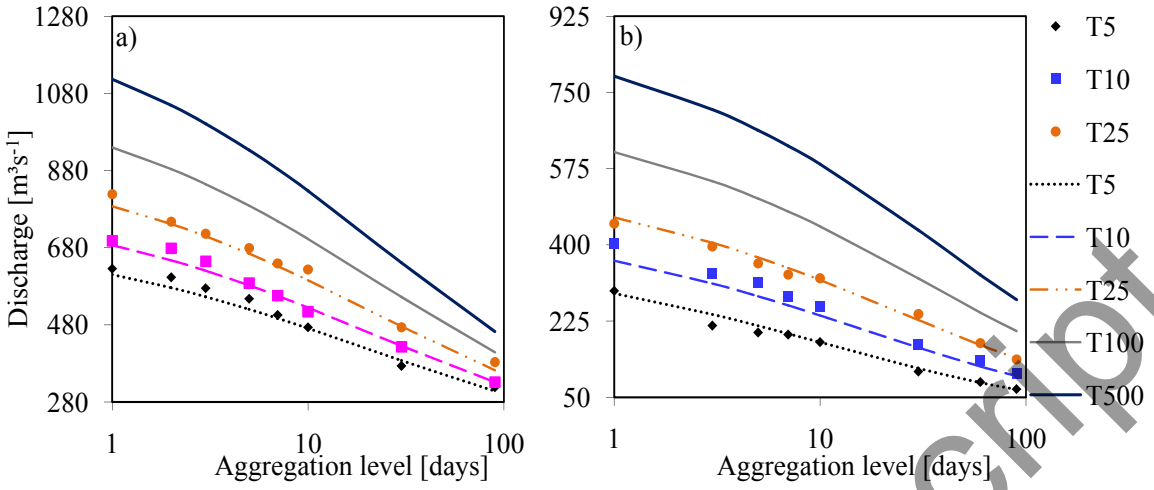

Figure 5 Calibration results of peak flow QDF relationships for a) Nzoia river (station 1EF01) and b) Nyando river (station 1GD01). The graphs share same label for the vertical axis. The legend entry e.g. *T*5 denotes *T*-year curve for $T = 5$ years.

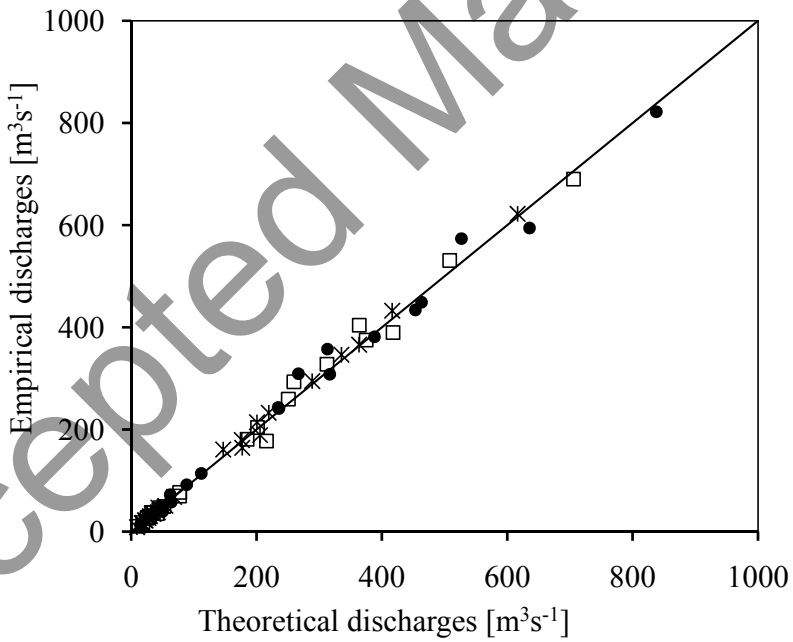

Figure 6 Evaluation of QDF calibration results for daily high flows of all selected catchments for return periods of 5, 10 and 25 years denoted by symbols (◊), (*) and (●) respectively.

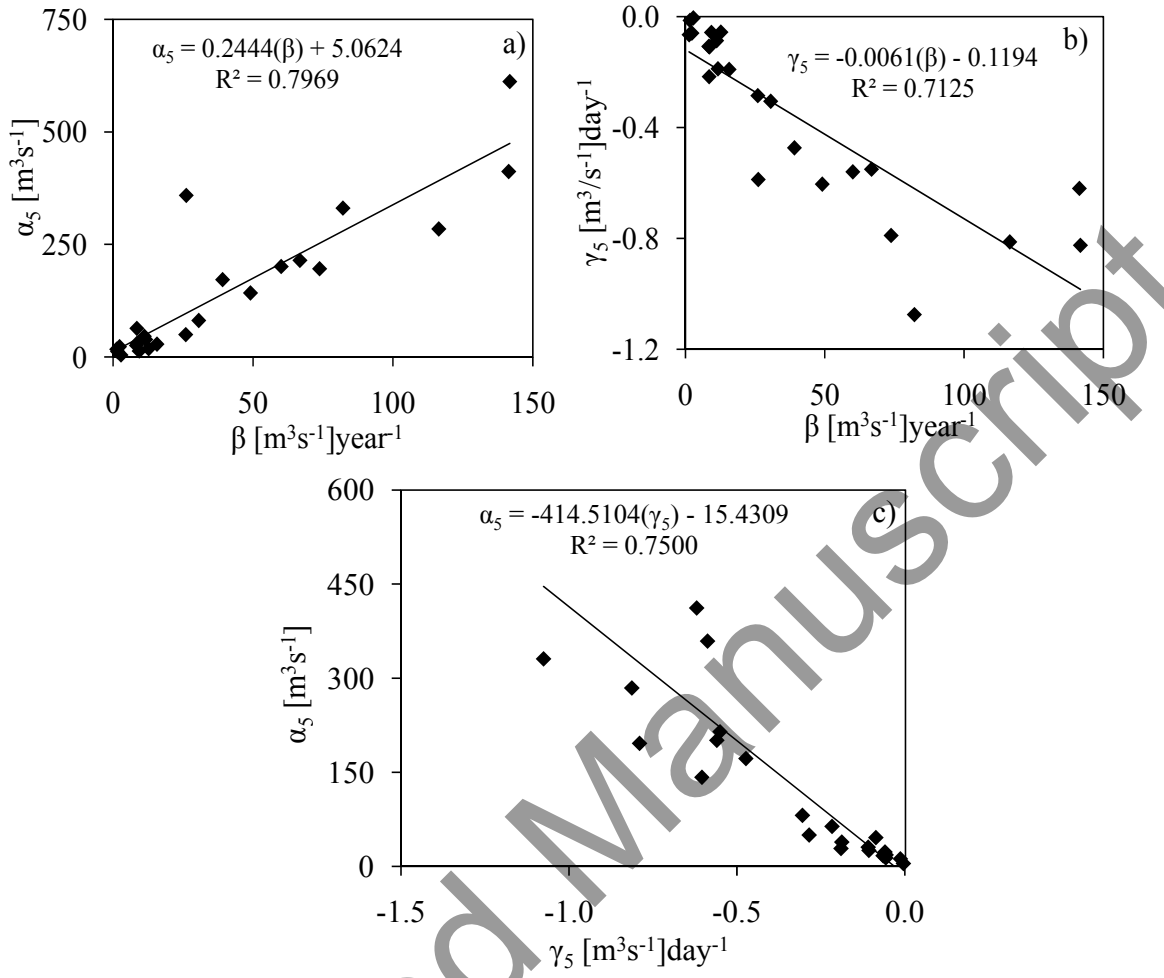

Figure 7 Relationships between the QDF parameters α_5, γ_5 and β.

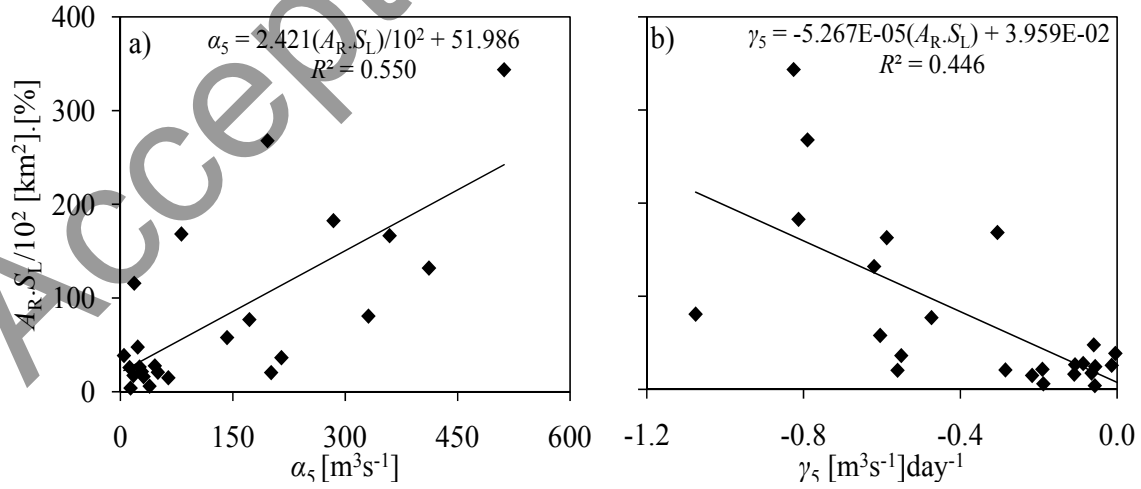

Figure 8 Relationships of the combined physiographic characteristic [$A_R.S_L$] with QDF parameters α_s and γ. Both graphs share same range and label for the vertical axis.

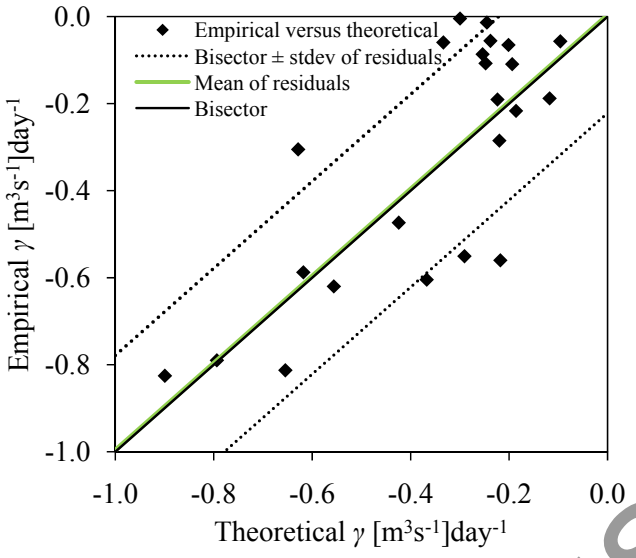

Figure 9 Evaluation of the calibration results of the regional regression model.

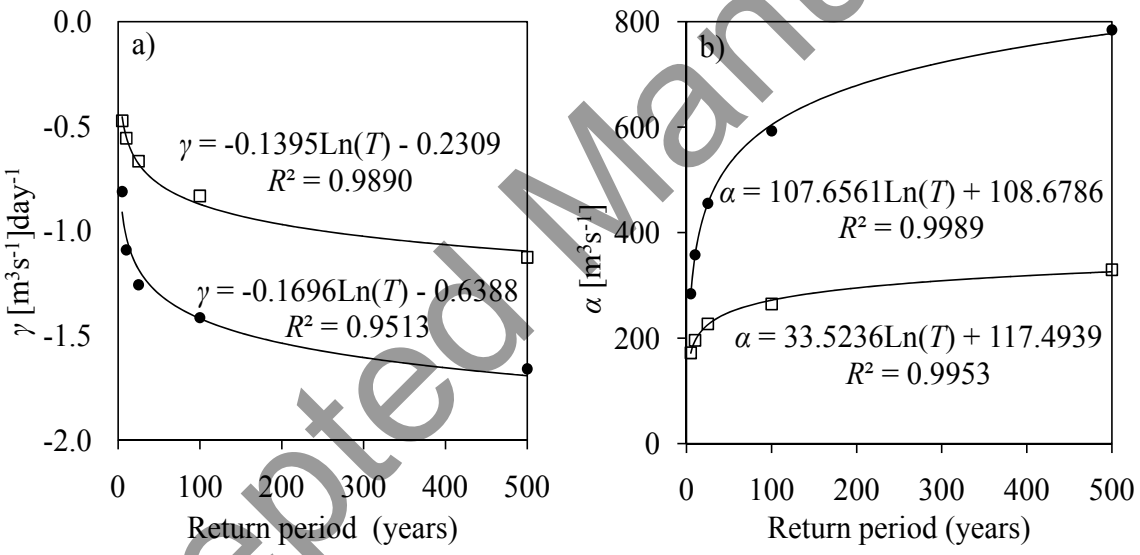

Figure 10 Variation of QDF parameters γ and α_s with return period. The symbol (●) is for Nyando river (station 1GD01) while (□) is for Yala river (station 1FG01).

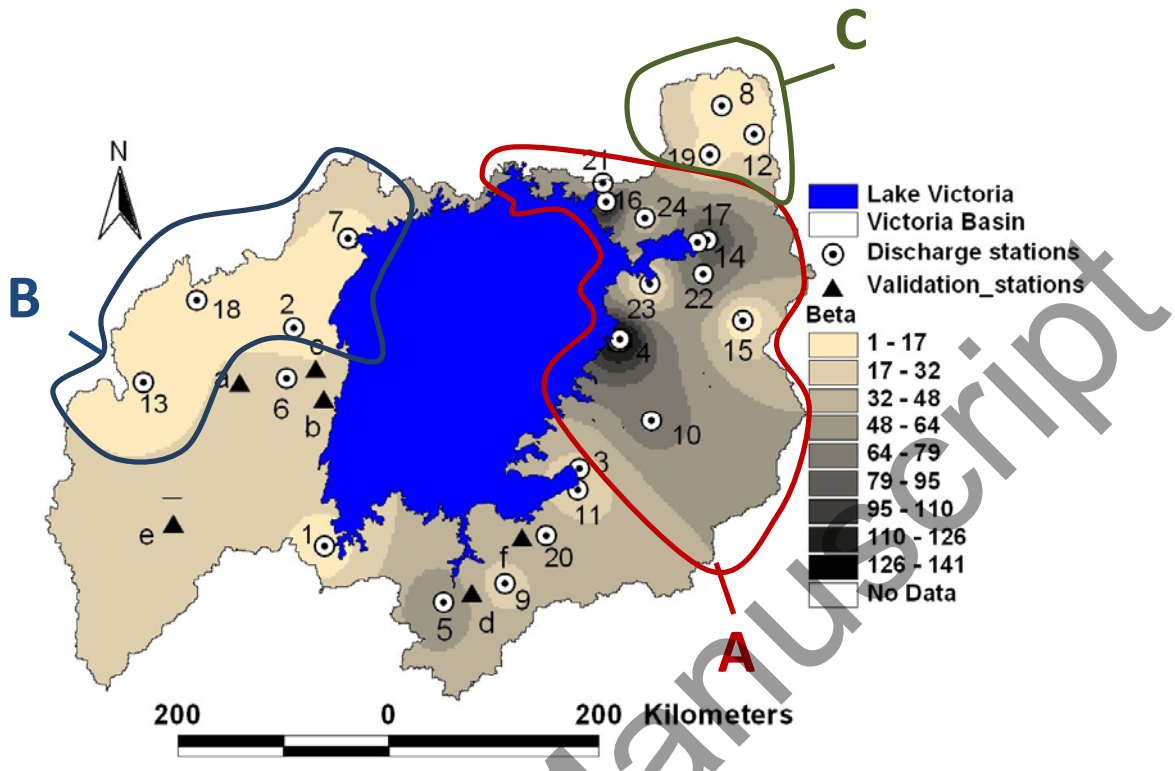

a)

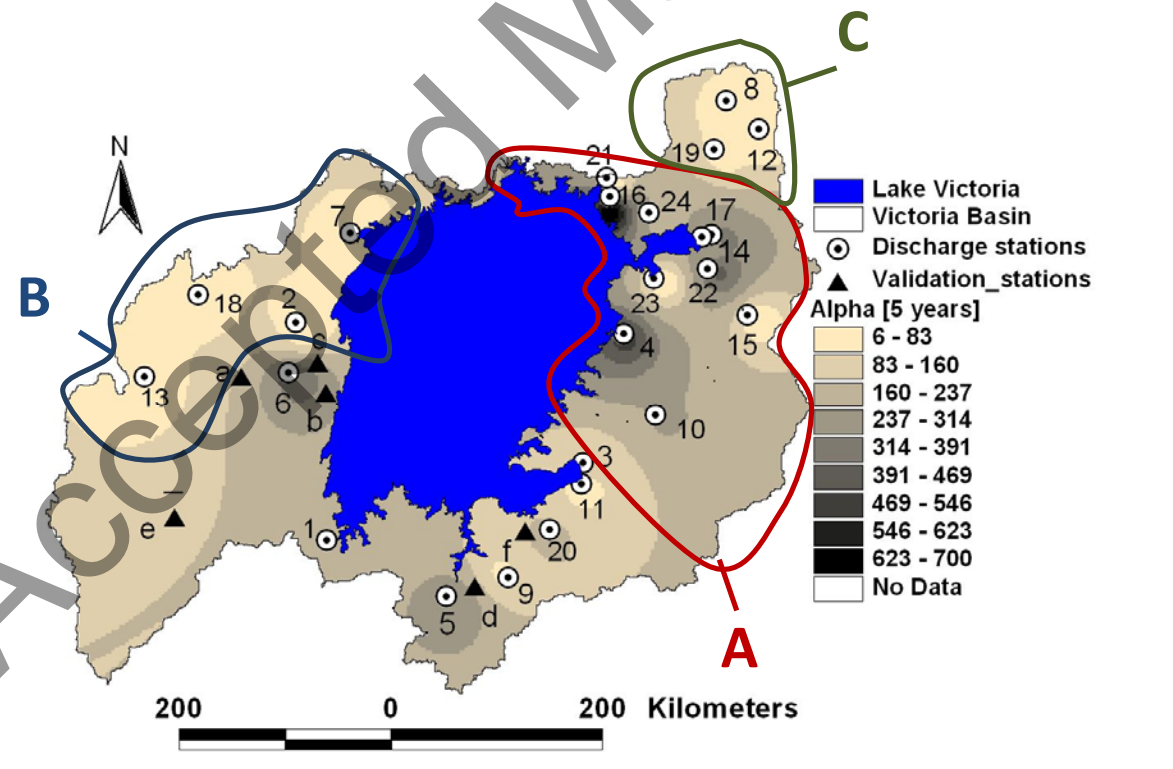

b)

Figure 11 Spatial maps showing regional differences in terms of; a) β, b) α_s for $T = 5$ years

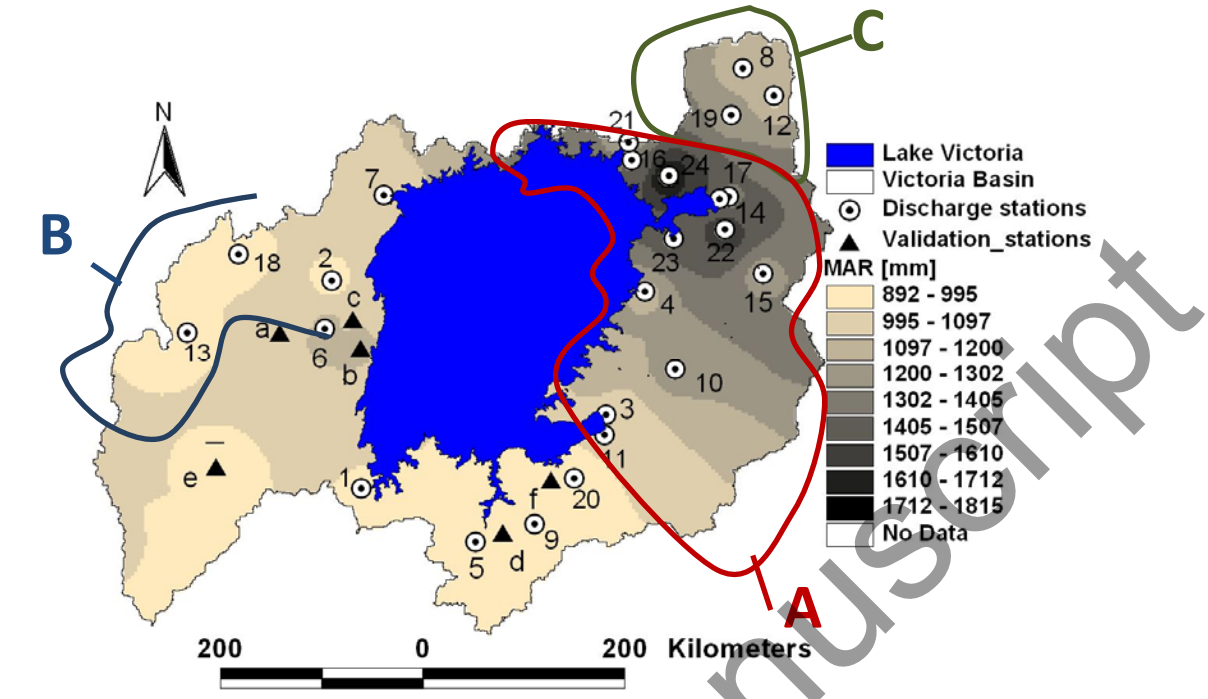

a)

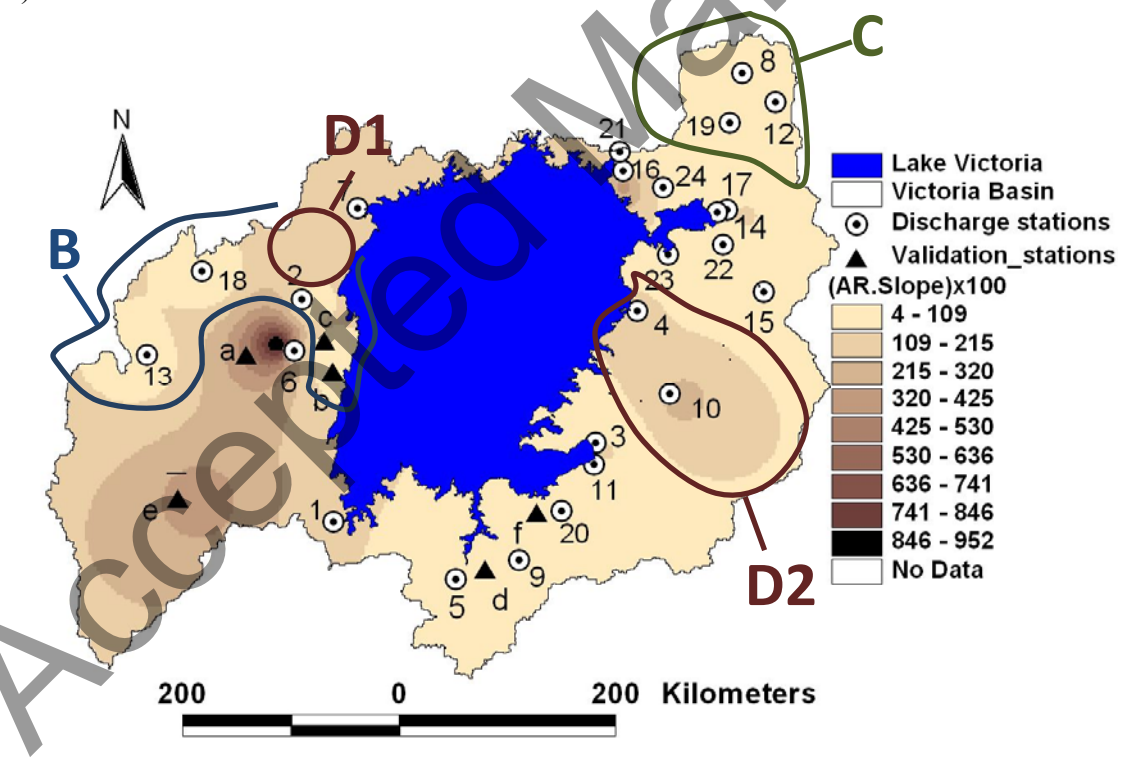

b)

Figure 12 Spatial maps showing regional differences in terms of; a) R_{AM} and b) $A_R.S_L$.

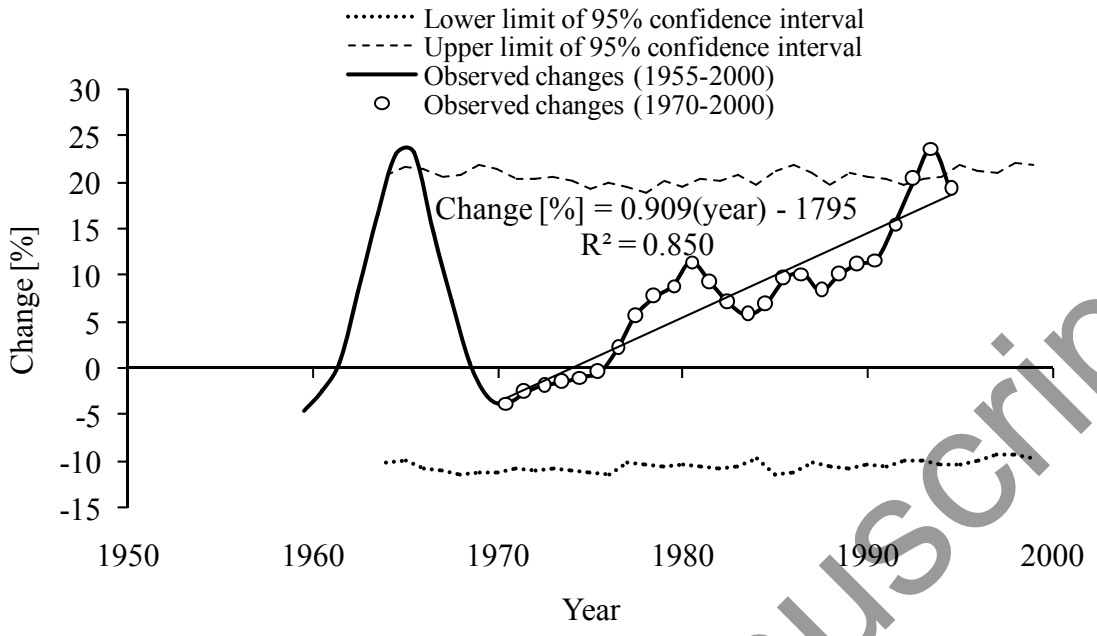

Figure 13 Temporal variability in the mean of annual maxima of LVB river flows for the period 1955–2000 using a time slice of 5 years.

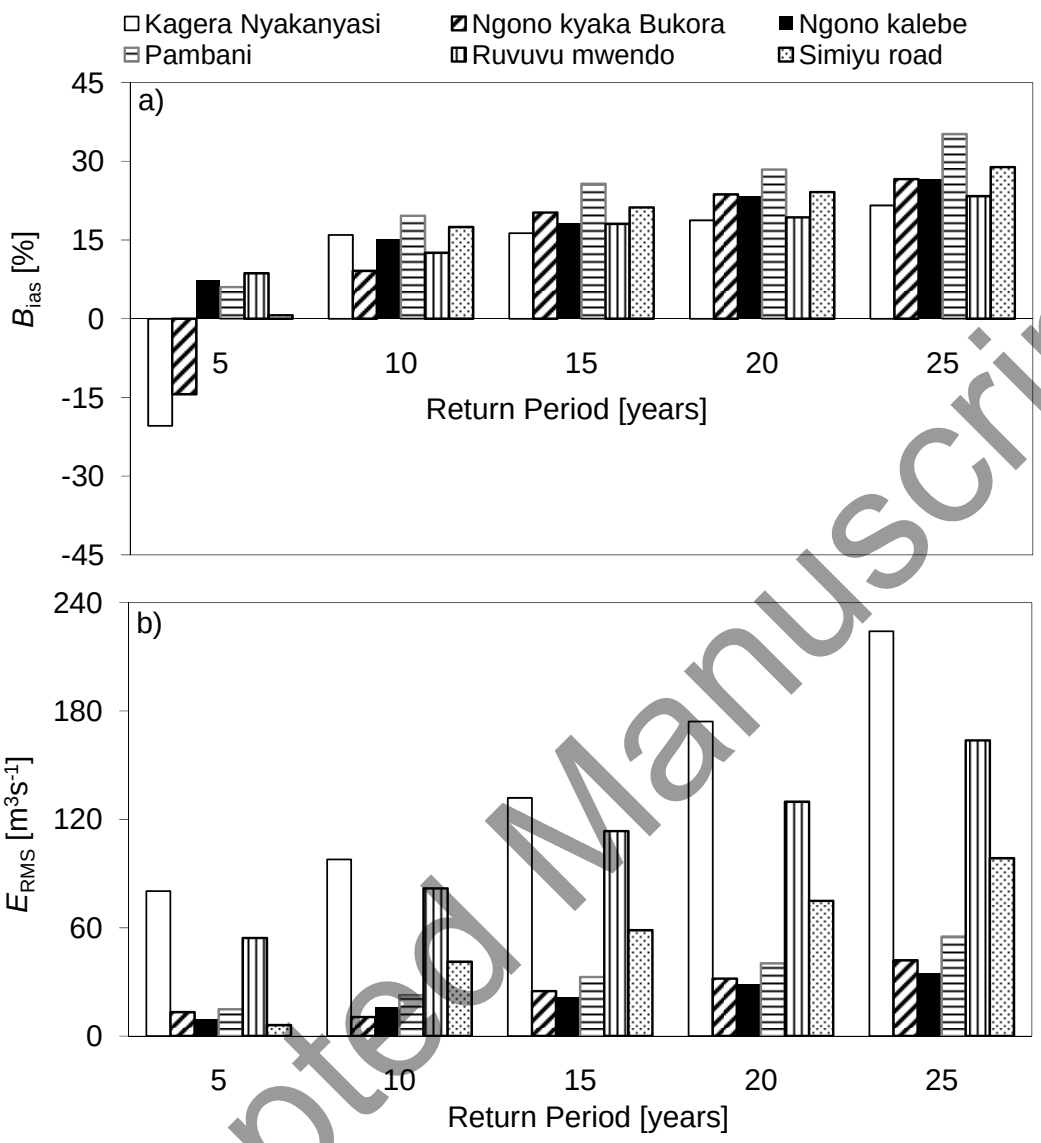

Figure 14 Evaluation of QDF regional models for return periods of 5, 10, 15, 20 and 25 years; a) B_{ias} [%], and b) E_{RMS} [m^3s^{-1}] of T-year flow estimates.

Table 1 Details of selected stations and their characteristics.

No.	Selected catchments	Station ID	Area [km^2]	Data length From	to	Location Long. [deg.]	Lat. [deg.]	Point SL[%]	Mean flow [m^{3}s^{-1}]
1)	Biharamulo	***	1981	1950	2004	31.29	2.62	1.40	18.2
2)	Bukora	81270	8392	1951	1976	31.48	-0.85	0.46	3.1
3)	Grumeti	5F3	13363	1950	2004	33.94	-2.06	1.60	11.2
4)	Gurcha-migori	1KB05	6600	1950	2004	34.20	-0.95	2.00	57.7
5)	Isanga	114012	6812	1976	2004	32.77	-3.21	0.30	29.7
6)	Kagera	58370	54260	1950	1994	31.43	-1.29	3.00	266.3
7)	Katonga	100006	15244	1950	1975	31.95	-0.09	0.76	5.1
8)	Koitobos	1BE06	813	1949	1975	35.09	0.97	2.15	3.2
9)	Magogo-maome	113012	5207	1950	2004	33.15	-2.92	0.40	7.8
10)	Mara	107072	13393	1950	2003	34.56	-1.65	2.00	37.3
11)	Mbalangeti	111012	3591	1950	2004	33.86	-2.22	0.60	4.3
12)	Moiben	1BA01	188	1953	1990	35.44	0.80	2.13	1.3
13)	Nyakizumba	100005	359	1950	1987	30.08	-1.32	4.01	4.7
14)	Nyando	1GD01	3652	1962	2001	35.04	-0.10	5.00	20.3
15)	Nyangores	1LA03	4683	1963	1993	35.35	-0.79	1.02	8.3
16)	Nzoia	1EF01	12676	1974	1999	34.08	0.13	2.01	115.4
17)	Ogilla	1GD03	2650	1970	1996	34.96	-0.13	1.37	16.5
18)	Ruizi	100004	2070	1970	1998	30.65	-0.62	0.29	3.8
19)	Sergoit	1CA02	659	1959	1990	35.06	0.63	2.46	2.3
20)	Simiyu Ndagalu	5D1	1205	1970	1996	33.56	-2.63	0.50	11.8
21)	Sio	1AH01	1450	1958	2000	34.15	0.38	1.03	11.4
22)	Sondu	1JG01	3508	1950	1990	35.01	-0.39	2.30	43.3
23)	South Awach	1HE01	3156	1950	2004	34.54	-0.47	0.82	6.0
24)	Yala	1FG01	3351	1950	2000	34.51	0.09	2.30	37.3
Validation stations									
a)	Kagera Nyakanyasi	5A13	48427	1970	1978	31.20	-1.18	1.97	228.8
b)	Ngono kalebe	5A3	1161	1970	1978	31.67	-1.41	0.81	15.3
c)	Ngonokyaka /Bukoba	5A1	3200	1978	1989	31.60	-1.23	0.47	23.0
d)	Pambani Mabuki Bridge	113022	1595	1970	1981	33.11	-2.97	1.11	2.33
e)	Ruvuvu Mwendo	5A16	10970	1970	1977	30.56	-2.47	2.18	103.8
f)	Simiyu Mwanza road	5D3	10200	1990	2001	33.45	-2.59	0.58	26.9

*** Missing Station ID Long.: Longitude Lat.: Latitude SL: Slope

Table 2 The overall average B_{ias} [%] and E_{RMS} [m^{3}s^{-1}] for the calibrated T-year flow quantiles considering the full range of aggregation levels.

	T_5	T_{10}	T_{25}
B_{ias} [%]	-0.38	-0.58	-0.78
E_{RMS} [m^{3}s^{-1}]	4.93	16.16	19.33
E_F [-]	0.995	0.994	0.993

Table 3 R^2 for relationships between the QDF parameters α_s, γ and β and individual possible predictors; α_s and γ are for a return period of 5 years.

	R_{AM}	A_R	S_L	E_{LEV}	D_L	A_{SP}	E_{MAT}
α_s	0.203	0.156	0.083	0.042	0.071	0.276	0.042
γ	0.220	0.072	0.091	0.007	0.065	0.203	0.110
β	0.140	0.007	0.179	0.004	0.097	0.171	0.065

Table 4 R^2 for relationships between the QDF parameters α_s, γ and β and possible combined predictors; α_s and γ are for a return period of 5 years.

	$R_{AM}.A_R$	$R_{AM}.S_L$	$A_R.S_L$	$E_{LEV}.A_{SP}$	R_{AM}.DL	$S_L.D_L$	$A_R.S_L.R_{AM}$	$A_R.S_L.E_{MAT}$
α_s	0.206	0.160	0.550	0.158	0.048	0.027	0.614	0.438
γ	0.098	0.193	0.397	0.082	0.035	0.020	0.444	0.307
β	0.017	0.262	0.484	0.065	0.075	0.018	0.527	0.235

Table 5 R^2 for relationships between the QDF parameters α_s and γ and combined predictors with increase in return period.

	T_5	T_{10}	T_{25}	T_{100}	T_{500}	T_5	T_{10}	T_{25}	T_{100}	T_{500}
	Model = $(A_R.S_L)$					Model = $(A_R.S_L.R_{AM})$				
α_s	0.550	0.524	0.506	0.483	0.308	0.614	0.585	0.565	0.539	0.493
γ	0.446	0.440	0.420	0.410	0.400	0.477	0.474	0.473	0.472	0.473
	Model = $a_0.(A_R.S_L)^{a1}$					Model = $a_0.(A_R.S_L.R_{AM})^{a1}$				
α_s	0.545	0.543	0.527	0.537	0.548	0.550	0.582	0.588	0.604	0.561
γ	0.506	0.551	0.561	0.568	0.523	0.550	0.582	0.588	0.604	0.561
	Model = $a_0.A_R^{a1}.S_L^{a2}$					Model = $a_0.A_R^{a1}.S_L^{a2}.R_{AM}^{a3}$				
α_s	0.620	0.618	0.602	0.612	0.623	0.655	0.646	0.615	0.581	0.534
γ	0.518	0.570	0.581	0.589	0.539	0.559	0.591	0.598	0.610	0.565

Table 6: Regional regression models for QDF parameter γ

Model	a_0	a_1	$\hat{R}^2$	E_F [-]	S_e $[m^3s^{-1}]day^{-1}$	E_{RMS} $[m^3s^{-1}]$
$a_0.(A_R.\ S_L)^{a1}$	-2.88E-01	5.03E-01	0.4834	0.5258	0.0463	0.2170

Table 7 The overall B_{ias} [%] and E_{RMS} $[m^3s^{-1}]$ for T-year flow estimates computed as average value considering all six validation stations and considering the full range of aggregation levels.

T [years]	5	10	15	20	25
B_{ias} [%]	-2.01	14.98	19.96	22.96	27.04
E_{RMS} $[m^3s^{-1}]$	29.61	44.91	63.76	79.83	102.95